Electronic Supplementary Material (ESI) for New Journal of Chemistry.

Supplementary Information

A facile, solid-state reaction assisted synthesis of berry-like $NaNbO_3$ perovskite structure for binder-free, highly selective sensing of dopamine in blood samples

Lignesh Durai[1], and Sushmee Badhulika[1*]

[1]*Department of Electrical Engineering, Indian Institute of Technology, Hyderabad, 502285, India.*

[*]*Corresponding author: E-mail: sbadh@iith.ac.in; Telephone: +040-23018443*

Morphological, Structural and Composition Analysis of Nb_2O_5

The SEM image shown in the Fig. S1 describes the morphology of the niobium pentoxide (Nb_2O_5) nanopowders obtained though the as synthesised solvothermal technique. The Fig S1(a) shows the massive agglomeration of the Nb_2O_5 nanoparticles as a microstructure and this was much clearly supported by the magnified image shown in fig. S1(b). The particle remains to be spherical in shape and the size of the particle remains ~10 to ~30nM as it get agglomerated to grow into micrometres structures. Fig. S1(c) displays the XRD pattern which confirms the amorphous Nb_2O_5 nanomaterial [1-3]. This is because the particles could not change into crystal under this temperature. Fig. S1(d) shows the Raman spectra of the Nb_2O_5 nanoparticles where the intense band found at 695cm^{-1} corresponds to the symmetric stretching of Nb-O (v_1) along with the shoulder peak found around the 330cm^{-1} corresponds to the Nb-O-Nb linkage and the low intense peak found at 465cm^{-1} indicates the $v_5(T_{2g})$ mode [4]. These structural and chemical analysis proves that there are no adequate traces of impurities of the precursors found at the end product of Nb_2O_5 nanopowders. Hence it has been used in the synthesis of $NaNbO_3$

through SSR without any further purification process. Fig. S1(e) depicts the FTIR spectrum of Nb_2O_5. The symmetric bending of Nb-O-Nb polyhedral was ascribed with the broad peak observed at 603 cm^{-1}[5]. The hexagonal formation of Nb_2O_5 was witnessed with the presence of sharp peak at 810 cm^{-1} which can also be attributed to O-Nb-O bending [6]. The OH molecules were observed with the presence of peaks at 1550cm^{-1} and 3329 cm^{-1} [7,8]. Fig. S1(f) shows the CV response of Nb_2O_5 nanopowder modified GCE towards the electrooxidation of DA in comparison with $NaNbO_3$/GCE and bare GCE. The response of the $NaNbO_3$/GCE was witnessed to be more prominent than the Nb_2O_5/GCE due to the presence of NbO_6 octahedra whereas Nb_2O_5 displayed only a mild reduction peak at ~0.07V. Hence, the enhancement in the response of $NaNbO_3$/GCE towards the DA was ascribed to the presence of the octahedral sites.

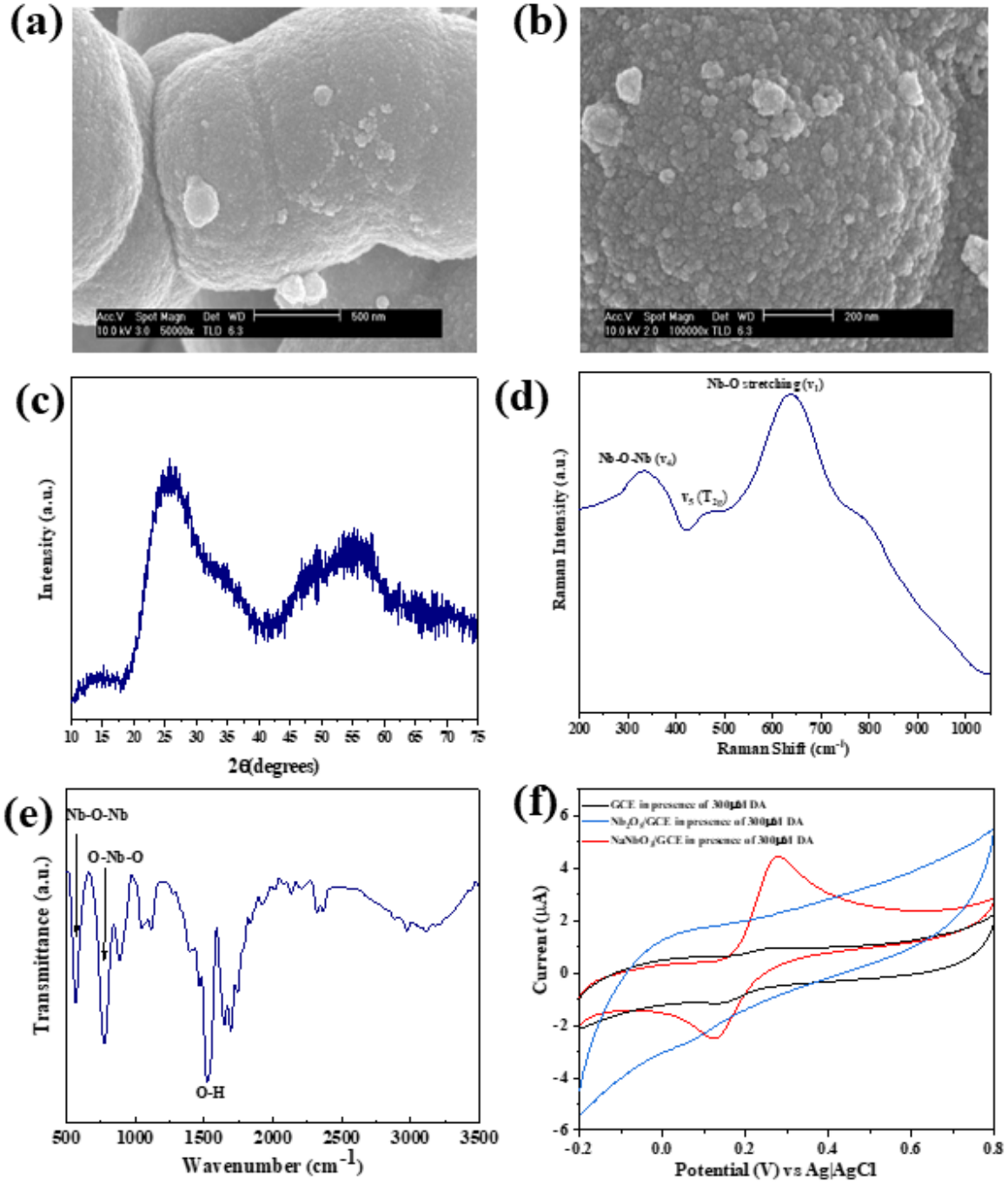

Figure S1: (a) SEM Images of Nb_2O_5 nanopowder (b) magnified SEM image of the Nb_2O_5 nanopowder (c) XRD pattern and (d) Raman spectra of the Nb_2O_5 nanopowder (e) FTIR spectra of Nb_2O_5 nanopowder (f) Typical CV response of Nb_2O_5/GCE, $NaNbO_3$/GCE and Bare GCE in presence of 300μM DA

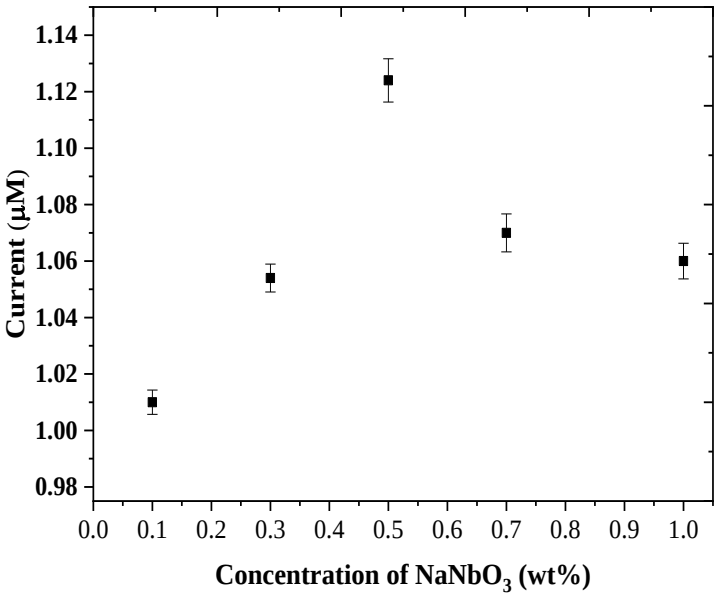

Figure S2: Oxidation peak current response of 0.1, 0.3, 0.5, 0.7 and 1wt% of the $NaNbO_3$/GCE in the presence of a 10μM DA (N = 3 devices).

The study on impact of electrolyte pH on electrooxidation of DA and to determine the optimal pH value of 0.1M PBS electrolyte for sensing, the CV of $NaNbO_3$/GCE was investigated at different pH from 7.0 -7.4 pH as shown in the fig. S3(a). The corresponding oxidation peak current versus pH was obtained as shown in fig. S3(b). There was a linear increase in the oxidation current as the pH increased from 7.0 to 7.2pH and the highest peak current was observed at 7.2pH beyond which there was a significant decrease in oxidation peak current which indicates the proton involvement in the DA redox reaction [9]. Fig. S3(c) shows the effect of pH on the oxidation potential of DA with a linear regression equation as y = 0.0395x-0.976(R^2=0.997) with a slope of 39mV/pH which confirms the equal number of electrons and proton in the DA redox reaction. Additionally, the optimized 7.2 pH mimics the biological conditions, hence it was used as supporting electrolyte for all successive experiments.

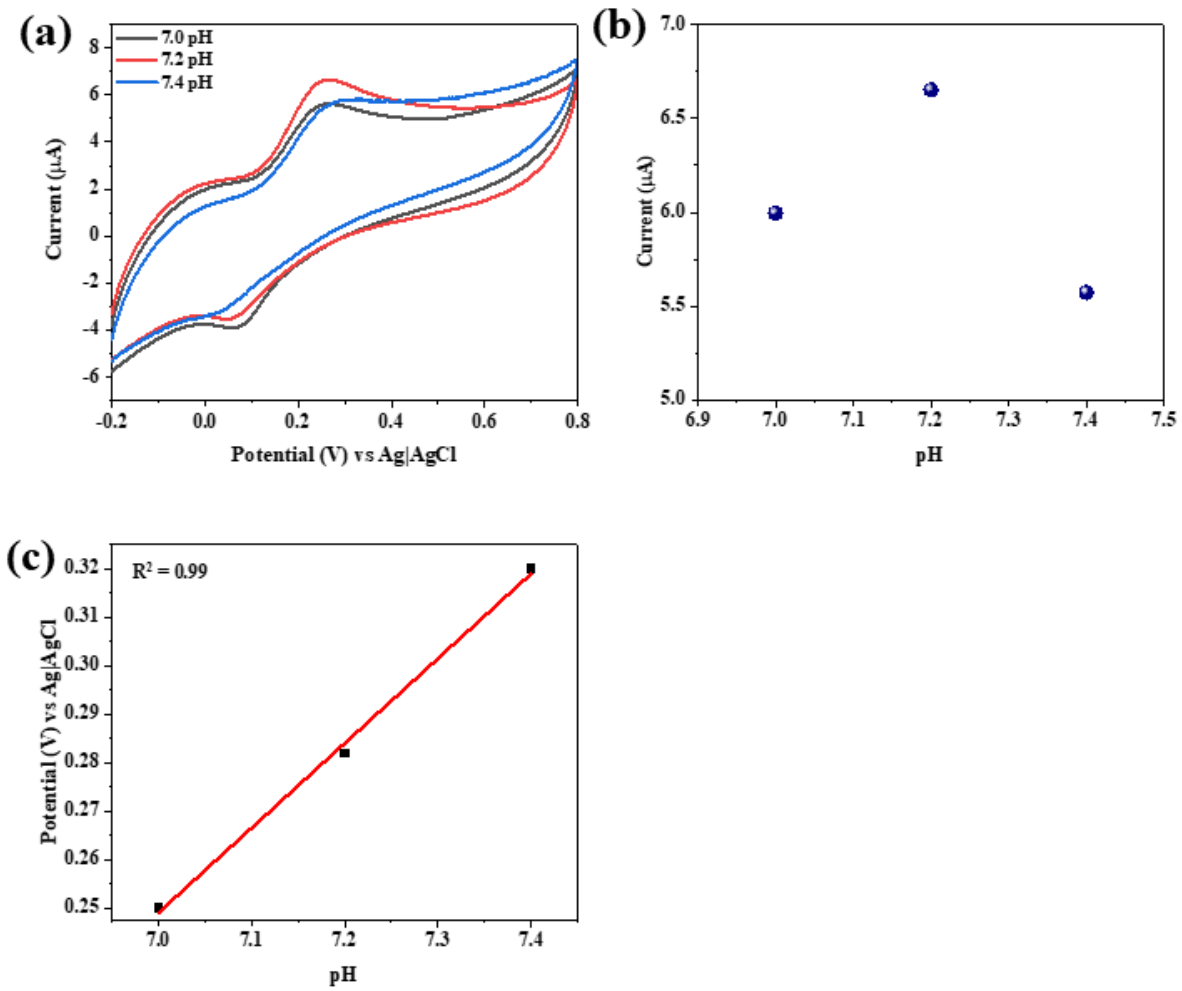

Figure S3: (a) CV of $NaNbO_3$/GCE electrode in 0.1 M PBS at different pH levels; (b) Effect of pH on the oxidation peak current (c) Effect of pH on the oxidation potential

Table S.1 Interference study of $NaNbO_3$/GCE towards DA sensing with possible interfering species.

S.No.	Interference	Concentration μM	Change in peak current (%)
1.	AA	40	3.36
2.	UA	40	1.93
3.	Na+	40	1.58
4.	Cl-	40	1.64
5.	Ca	40	1.30
6.	Glucose	40	4.98

References

[1] R. F. Brandão, R. L. Quirino, V. M. Mello, A. P. Tavares, A. C. Peres, F. Guinhos, J. C. Rubim and P. A. Suarez, *J. Braz. Chem. Soc.*, 2009, **20(5)**, 954-966.

[2] S. Venkataraj, R. Drese, C. Liesch, O. Kappertz, R. Jayavel and M. Wuttig, *J. Appl. Phys.*, 2002, **91(8)**, 4863-4871.

[3] S. Li, Q. Xu, E. Uchaker, X. Cao and G. Cao, *CrystEngComm*, 2016, **18(14)**,2532-2540.

[4] R. R. Pereira, F. T. Aquino, A. Ferrier, P. Goldner and R. R. Gonçalves, *J. Lumin.*, 2016, **170**, 707-717.

[5] X. Jin, C. Liu, J. Xu, Q. Wang and D. Chen, *RSC Adv.*, 2014, **4(67)**, 35546-35553.

[6] T. Athar, A. Hashmi, A. Al-Hajry, Z. A. Ansari and S. G. Ansari, *J. Nanosci. Nanotechnol.*, 2012, **12(10)**, 7922-7926.

[7] L. Yan, G. Chen, S. Sarker, S. Richins, H. Wang, W. Xu, X. Rui and H. Luo, *ACS Appl. Mater. Interfaces*, 2016, **8(34)**, 22213-22219.

[8] A. K. Das, M. Srivastav, R. K. Layek, M. E. Uddin, D. Jung, N. H. Kim and J. H. Lee, *J. Mater. Chem.*, 2014, **A 2(5)**, 1332-1340.

[9] X. Ma, M. Chao and Z. Wang, *Anal. Methods*, 2012,**4**, 1687-1692.